Revisiting trajectory analysis - Evolving the Cranfield model

Matthew Greaves (MO5700)
Safety and Accident Investigation Centre, Cranfield University

Matthew Greaves is a Senior Lecturer in the Safety and Accident Investigation Centre at Cranfield University. Prior to joining Cranfield, he worked for the science and technology organization QinetiQ. He holds an engineering degree and a Ph.D. in aircraft engine noise and vibration. His research deals with the application of technology to the accident investigation process and he is an ESASI committee member.

Introduction

One of the problems faced by air accident investigators is that of aircraft suffering in-flight breakup. Such breakups can be caused by a number of mechanisms including mid-air collision, disintegration or detonation of explosives, with high profile examples including the sabotage of Pan Am 103 over Lockerbie [1] and the explosion of flight TWA 800 over the Atlantic Ocean [2]. In both events, trajectory analysis was employed in an attempt to understand certain aspects of the accident.

As an example, often in cases of in-flight breakup, questions exist about the position of the aircraft prior to breakup including altitude, speed, heading etc. An alternative scenario exists when aircraft are lost, as was the case with Adam Air Flight 574 [3], which disappeared from radar over Indonesia and remained unlocated for 9 days until small parts of wreckage were found. In such cases, it could be useful to know the possible search region assuming a catastrophic event occurred between radar returns. A third example exists when searching for a specific piece of wreckage which will aid the investigation, such as in the uncontained fan disk failure of flight UA 232 which crash-landed at Sioux City [4]; despite being a crucial piece of evidence, the fan was not discovered until 3 months after the accident. Trajectory analysis is suitable for application to all of these and many other accidents.

This paper describes work to develop a new generation of trajectory model which will incorporate effects of altitude dependent gravity and air density. It also presents a new approach to wind modelling. The model is solved using a robust numerical scheme and sample results are presented regarding the sensitivity of components to initial condition errors.

Literature review

There is a large historical body of work around trajectory analysis [5-18]. More recently, trajectory analyses have also been conducted for a number of other significant accidents including TWA 800 [19], Air India AI182 [20] and China Airlines CI611 [21].

Work on trajectory analysis began at Cranfield in 1978, in participation with the UK Accidents Investigation Branch, to develop a computerized method for calculating trajectories. The TRAJAN (TRAJectory ANalysis) model was born out of work done and reported as MSc theses by Khan [22], Hull [23] and most significantly, Steele [24]. This work was later reviewed and developed by Anker and Taylor and formed the basis of the model which was used for analysing the Lockerbie accident in 1988 [25, 26, 27].

TRAJAN is a time-stepping code using a constant timestep and assuming linear behaviour across the timestep. As a result of its era, the program provides no graphical output; in 1978 graphical output was extremely hard to produce with the first Graphical User Interface (GUI) not appearing until 1981. However, the study of trajectories is one that is often most easily

understood through visualisation. Therefore, the TRAJAN output was often used to produce graphs and curves. In addition, ground maps were sometimes produced, to scale, on acetate for overlay on Ordnance Survey maps. Again, this is representative of the time of development. Computing technology and the availability of digital mapping mean that this aspect should be easy to improve on in a modern implementation.

Model development

The problem of developing an analysis model is essentially one of calculating ballistic trajectories. Whilst the investigator is clearly interested in more than the path taken by a part falling to ground, if the trajectory is fully understood then other variables such as initial velocity, final velocity, time to fall to earth, impact velocity, aerodynamic force etc. are also directly available.

NATO and the US DOD define a ballistic trajectory as the "*trajectory traced after the propulsive force is terminated and the body is acted upon only by gravity and aerodynamic drag*." [28]. Clearly this definition is appropriate when considering wreckage created through midair breakup. Exceptions to this definition would include an aircraft which is damaged but still producing propulsive force and components which are capable of generating lift. The latter point is an important one - in the subsequent analysis, the components will be considered to be acted on by drag alone; no lift force will be included. In addition, the 'tumbling' of parts whilst falling will also be discounted and instead replaced by a single drag coefficient.

Both of these assumptions are deviations from reality. Whilst they might accurately describe the behaviour of a high mass, compact body (one with a high value of ballistic coefficient - see later), a lighter part with a large area capable of producing lift (such as a section of fuselage skin with stringers) is clearly very likely to produce lift and tumble as it falls such as a sheet of cardboard might do if dropped.

Any trajectory model must depend upon some estimation of the drag coefficient of the part, which is often difficult to achieve. This is compounded by the fact that when objects tumble they effectively present a variable drag coefficient. Given the unavoidable inaccuracies inherent in drag coefficient estimation, it is arguable whether a more advanced calculation technique is necessary. However, there is no reason not to minimize as many errors as possible, as long as the other inaccuracies and limitations are understood.

When ignoring wind and air resistance, the theory behind trajectories of idealized projectiles is simple and well understood. This is complicated slightly when including the effects of air resistance, although in some cases this is still easily solved.

However, an opportunity exists to develop a model which incorporates many of the more subtle effects necessary for it to be widely applicable. These include: full three-dimensional effects of wind; effects of atmospheric density changes; and the variation of gravity with height. These effects are particularly important if very high altitude accidents, such as the Columbia (STS-107) or Challenger (STS-51-L) space shuttle accidents are to be analysed. At present, the rotation of the earth is not considered.

One-dimensional derivation

At its most simple, assuming one-dimensional (x) vertical motion, drag proportional to velocity squared (v^2), assuming constant mass (m) and gravity (g) and ignoring wind effects, gives the governing differential equation of

$$m\frac{dv}{dt} = mg - \frac{1}{2}\rho C_D S v^2 \qquad (1)$$

where

$$v(t) = \frac{dx}{dt},$$

S is frontal area, C_D is drag coefficient and ρ is density, which can be solved for $v(t)$ and $x(t)$. This is Newton's Second Law, with the forces acting on the body on the right hand side of the equation and the resulting acceleration on the left hand side. In order to expand this simple model to incorporate the more complex aspects, it is necessary to quantify and model the effects and variations of each of the components.

The ICAO standard atmosphere [29] allows the variation of gravity with altitude to be written as

$$g = g_0\left(\frac{r_e}{r_e + h}\right)^2$$

where r_e is the nominal radius of the earth, taken as 6,356,766 m and *h* is geometric altitude. The ICAO standard atmosphere also gives governing expressions for the variation of air density with geometric altitude for the two temperature gradient regimes as

$$\rho = \frac{p_b}{RT_b}\left[1 + \frac{\beta}{T_b}\left(\frac{r_e x}{r_e + x} - H_b\right)\right]^{-(1+g_0/\beta R)} \qquad \text{for } \beta \neq 0$$

and

$$\rho = \frac{p_b}{RT}\exp\left[-\frac{g_0}{RT}\left(\frac{r_e x}{r_e + x} - H_b\right)\right] \qquad \text{for } \beta = 0$$

where p is the atmospheric pressure, β is the temperature gradient, T is the temperature, H is geopotential altitude and R is the specific gas constant. The subscript b indicates the given value evaluated at the lower limit of the layer of concern.

It is worth noting that the ICAO standard atmosphere is valid up to 'only' 262,500 ft (80km). Whilst this is many times the normal cruising altitude of commercial aircraft it does not encompass the full range of altitudes that may be seen by spacecraft operating in the atmosphere. For example Virgin Galactic plan to take SpaceShipOne to 360,000 ft (100 km) [30]. This is not a significant limitation and can be easily adapted, but it should be noted before making high altitude predictions.

Drag force is assumed in equation (1) to be the form of $0.5\rho C_D S v^2$. This is a well-established approach [e.g. 31], however it is important to note that the velocity described is the square of the component's airspeed not its groundspeed. This is because the drag is created by the relative airflow; a particle travelling at precisely the windspeed in theory experiences no drag.

In order to provide a full solution to the trajectory problem which incorporates wind data, it is necessary to provide some function which accurately describes the variation of wind speed (in this 1D case, acting vertically) with altitude. This subject will be returned to, but for now it is sufficient to assume that such a function, $W_x(x)$ is available. The wind appears in the drag calculation, and it is this effect that causes the particle to adopt the surrounding windspeed.

Combining all of these effects - variable gravity, variable density, and the expression to describe wind - allows Equation (1) to be modified to

$$m\frac{dv_{GND}}{dt} = mg(x) - \frac{1}{2}\rho(x)C_D S v_{TAS}^2$$

where v_{TAS} is the true airspeed in the x direction and v_{GND} is the vertical speed relative to the ground. Incorporating the previously derived expressions, gives

$$m\frac{dv_{GND}}{dt} = mg_0\left(\frac{r_e}{r_e+x}\right)^2 - \frac{1}{2}\frac{p_b C_D S}{RT_b}\left[1+\frac{\beta}{T_b}\left(\frac{r_e x}{r_e+x}-H_b\right)\right]^{-(1+g_0/\beta R)} v_{TAS}^2 \qquad \text{for } \beta \neq 0$$

$$m\frac{dv_{GND}}{dt} = mg_0\left(\frac{r_e}{r_e+x}\right)^2 - \frac{1}{2}\frac{p_b C_D S}{RT}\exp\left[-\frac{g_0}{RT}\left(\frac{r_e x}{r_e+x}-H_b\right)\right] v_{TAS}^2 \qquad \text{for } \beta = 0$$

and

$$v_G = v_{TAS} + W_x$$

which are the differential equations governing the one-dimensional motion of a particle falling through the atmosphere. An attempt was made to solve this equation analytically, but whilst a solution may be possible, it quickly becomes intractable. For simplicity, from this point only the $\beta \neq 0$ solution will be used which restricts the use to the troposphere (11,000m). However, the approach outlined is equally applicable to both scenarios and the full atmosphere is available through this solution.

Three-dimensional expansion

Moving to a three-dimensional formulation, the position and velocity relative to the ground of a piece of wreckage is given by

$$\mathbf{r} = \begin{bmatrix} x \\ y \\ z \end{bmatrix} \qquad \text{and} \qquad \mathbf{v}_{GND} = \frac{d\mathbf{r}}{dt} = \dot{\mathbf{r}} = \begin{bmatrix} \dot{x} \\ \dot{y} \\ \dot{z} \end{bmatrix} = \begin{bmatrix} v_x^G \\ v_y^G \\ v_z^G \end{bmatrix}$$

where x, y and z are defined relative to the final aircraft track, with x directly along the aircraft track, y orthogonal to the aircraft track (when viewed from above, y increases to the left) and z being positive upwards. Introducing the ballistic coefficient, defined as

$$C_B = \frac{m}{C_D S}$$

is useful. There have been differing definitions of the ballistic coefficient with some using mass and others using weight (i.e. differing by a factor of 'g'). In this work, the mass definition given above will be used. The ballistic coefficient governs the aerodynamic drag behaviour of an object and offers a single parameter for classifying objects. An object with a high ballistic coefficient will have a high mass, low product of drag coefficient and frontal area, or both.

In order to incorporate wind data into the model, it is assumed that either measured wind data or 'aftercast' data are available, supplied at discrete altitudes. It is therefore necessary to choose an interpolation method in order to allow data to be obtained at altitudes other than those supplied. One option for representing the wind data is to assume constant windspeed in each band (which is equivalent to the 'zero order hold' technique of signal processing). This brings mathematical simplicity, but introduces problems at the transitions such as speed discontinuities which bring differentiation problems. This approach is also unlikely to accurately represent the true physical situation, unless the data points are very closely spaced. An alternative approach is to adopt linear interpolation between data points. This removes the discontinuity problem, although there may still be significant gradient transitions at data points.

It also provides, by definition, a precise fit to the supplied data points. However, linear interpolation offers no attempt to smoothly transition through data points - intuitively wind speeds are more likely to vary smoothly with altitude than with step changes in gradient. As with the constant assumption, linear interpolation is of more benefit where the data points are closely spaced. Ideally it would be possible to accurately fit a curve to all of the data points which can be simply described mathematically, such as a polynomial curve. However, whether this is possible depends on the data to which the curve is to be fitted. Figure 1 shows measured data for an arbitrary location and time, taken from the NOAA website [32]. The data presented is wind speed (ignoring direction at present) at a range of altitudes. This data is presented simply as a random sample of a wind profile to see what might be expected in terms of data, gradients etc. It is not intended to be representative of anything other than possible values. Examining Figure 1, it is apparent that neither the third-order nor the sixth-order polynomial curve accurately represent the measured data.

Because of the poor fit provided by the simple polynomials, an alternative approach is required. In this situation, a spline curve will be used. Spline curves use the supplied data points as control points for fitting a polynomial of some degree. The difference between fitting a polynomial, such as in Figure 1, and using a spline is that in the latter, the curve is constructed from many polynomial curves which are pieced together (so-called piecewise polynomial curves). This means that each polynomial curve is only attempting to fit to a small number of data points, rather than the entire data set, thereby allowing a much more precise fit. It is common to use a cubic polynomial as the basis for the spline since a cubic curve is the lowest degree of polynomial that can support an inflection. The typical form for the one-dimensional case is given as:

$$W(x) = w_0 + w_1 x + w_2 x^2 + w_3 x^3$$

Cubic curves are also very well behaved numerically. Therefore, in order to fit to the data, a cubic spline will be adopted which takes the measured data points as the reference points. In addition, the cubic spline can always be reverted to the linear interpolation or constant band assumptions described earlier, by setting constants in the expansion to zero. Figure 2 shows the cubic spline fit for orthogonal components for the random wind sample. The graph shows some difficulty in the cubic spline accurately representing smooth transitions from point to point without introducing data outside the shortest path however, it is a significantly closer fit than the third-order and sixth-order polynomials. Assuming that the wind does not vary with x and y location, then the following expression, which is a function only of z can be defined.

$$\mathbf{v}_{WIND}(z) = \begin{bmatrix} v_x^W \\ v_y^W \\ v_z^W \end{bmatrix} = \begin{bmatrix} a_x + b_x z + c_x z^2 + d_x z^3 \\ a_y + b_y z + c_y z^2 + d_y z^3 \\ a_y + b_y z + c_y z^2 + d_y z^3 \end{bmatrix} = \mathbf{a} + \mathbf{b}z + \mathbf{c}z^2 + \mathbf{d}z^3$$

In situations where the wreckage travels significant distances, or where the wind profile changes rapidly, the assumption of a constant wind profile will cease to be valid. A single profile is assumed in this case. Therefore, incorporating all of the variations into the three-dimensional expressions gives the governing vector equation,

$$\frac{d\mathbf{v}_{GND}}{dt} = \left(\frac{r_e}{r_e + z}\right)^2 \begin{bmatrix} 0 \\ 0 \\ -g_0 \end{bmatrix} - \frac{1}{2C_B}\frac{p_b}{RT_b}\left[1 + \frac{\beta}{T_b}\left(\frac{r_e z}{r_e + z} - H_b\right)\right]^{-(1+g_0/\beta R)} (\mathbf{v}_G - \mathbf{v}_{WIND})|\mathbf{v}_G - \mathbf{v}_{WIND}|$$

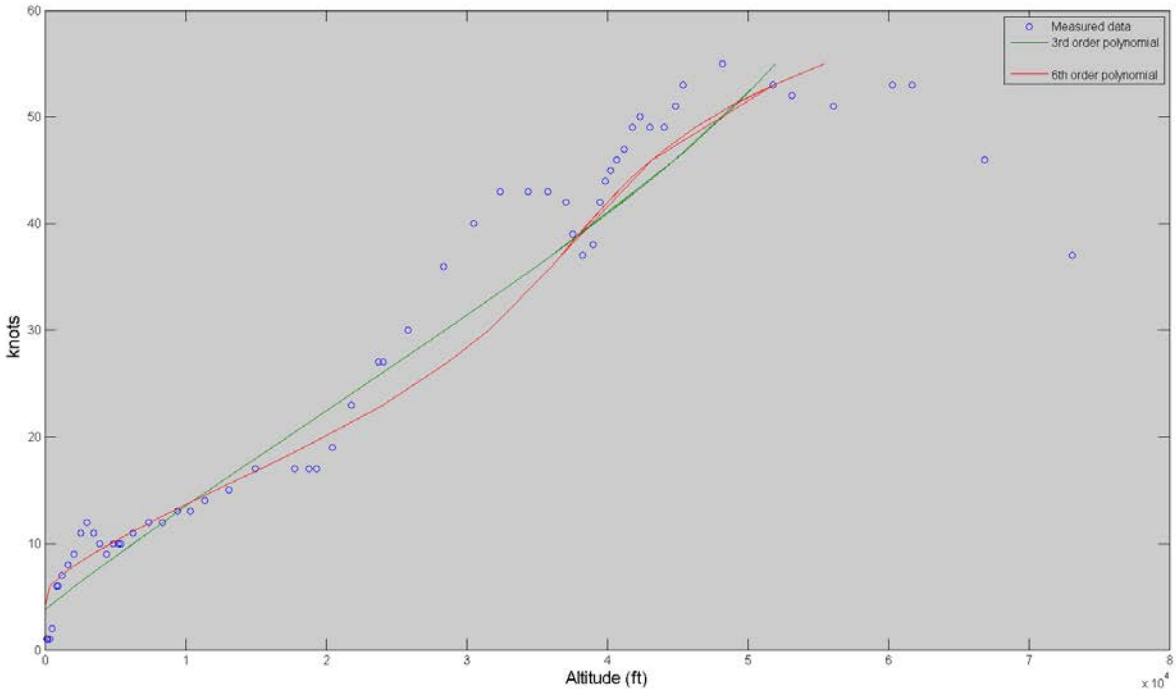

Figure 1 - Third order and sixth order polynomial fit to measured wind data

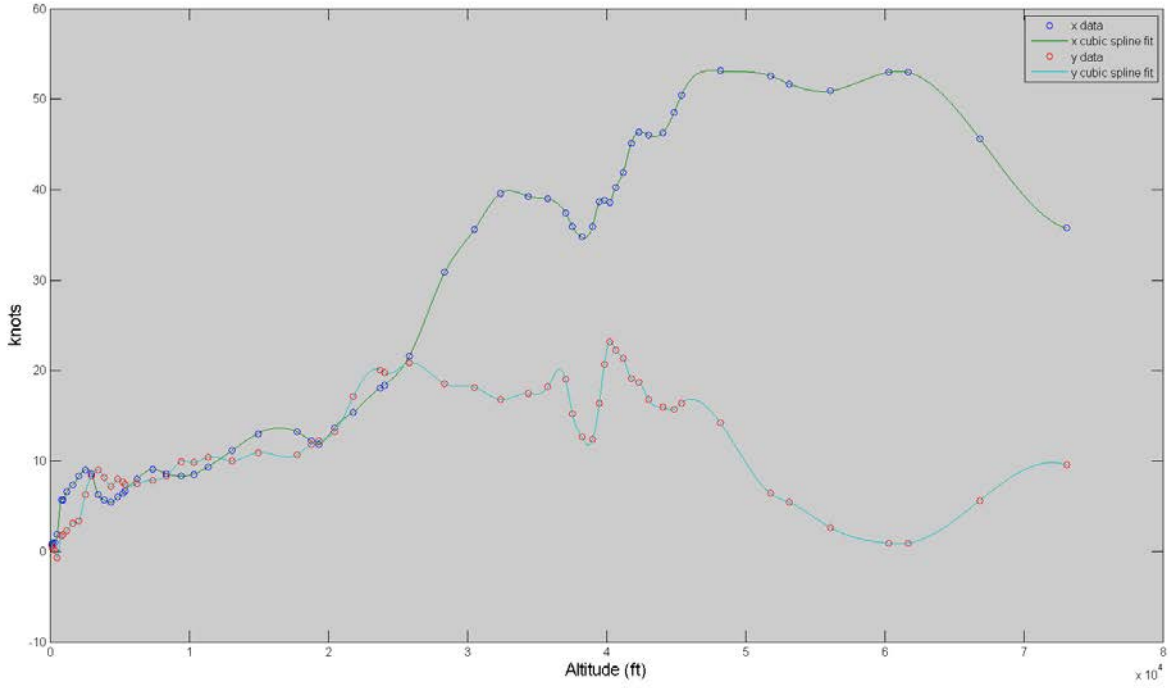

Figure 2 - Cubic spline fit for x and y components of wind data

Numerical solution

In order to solve the equation above, it is necessary to implement a numerical integration scheme. There are myriad integration schemes [see e.g. 33], with popular examples including , Euler, Runge-Kutta, Richardson extrapolation and predictor-corrector or multistep methods.

The linear, time-stepping approach adopted by TRAJAN is an example of the Euler method. It is an explicit (or forward), first-order scheme meaning that the solution at a point depends only on the points prior to that and that the truncation error is of the order of the timestep. However, the Euler method can be unstable, particularly with stiff equations (see below). Press et al. suggest that Euler's method is "*not* recommended for any practical use" [33].

The possibility of a system becoming 'stiff' arises as soon as more than one first-order ordinary differential equation (ODE) is involved. A stiff system of ODEs is one in which the ratio of the greatest eigenvalue to the smallest is much greater than one [34]. Eigenvalues are representative of the solutions to the ODEs, with a large eigenvalue representing a contribution to the solution which dies away quickly. It is this property that presents the difficulty of stiffness. By analyzing the numerical properties of the system it is possible to establish whether a system of equations is stiff or not. In this case, a stiffness ratio, SR (largest eigenvalue/smallest eigenvalue) of 5×10^7 was produced for a typical value set. Hall and Watt [35] suggest that a system is stiff if SR>>0, that if SR is of the order of 10 it may be considered to be marginally stiff, and that orders of 10^6 are not uncommon. Clearly, the trajectory problem derived here needs to be recognised as a stiff system and treated appropriately. A higher order implicit method was selected for this problem. Once implemented, the numerical solution was validated against analytical solutions without wind, and then against simplified examples including wind effects.

Results and discussion

Having validated the model, the numerical solution now provides the ability to calculate the trajectory of a particle given a set of initial conditions and wind data. Therefore, the model allows investigators to calculate potential trajectories based on the information they have available. However, whilst the model provides answers for the situation it is given, it provides no information about which factors are important in the behaviour of a given particle. Put differently, there is no 'sensitivity' information available - it is not clear whether changing, say, the initial velocity will induce a massive change in final ground impact position, or whether it will be almost inconsequential. For this reason, a form of sensitivity analysis will be conducted. When constructing this sensitivity analysis approach, it is important to be conscious of the desired final application, i.e. the study of aircraft breakups. Whilst it might be academically interesting to study, say, the variation in fall-time of a trajectory with changes in particle mass, this may be of little relevance to the problem of accident investigation, where normally the key information is at the point of ground impact. An exception to this may be in trying to match radar traces to a breakup sequence. However, such analysis can always be achieved by an individual investigator running a range of specific scenarios.

This analysis instead focuses on uncertainty levels. Faced with a given scenario, there is likely to be uncertainty around a number of different variables used in the analysis, including: wind speed and direction, initial position, initial velocity, drag coefficient etc. In trying to understand a particular set of events, an investigator may wish to vary certain variables through a range of values or improve the accuracy of certain parameters. However, establishing which parameters are likely to produce the greatest difference in ultimate wreckage location will be a process of trial and error.

The analysis takes two example initial conditions about which parameters will be varied by ±10% (or ±9° in the case of wind angle). This will allow a greater understanding of the key variables which may be required. It is worth noting that the problem in hand is highly nonlinear. This means that in practice, any results obtained for a specific problem set are valid for only that problem, and hence are not generalizable to all problems.

The two problem sets are:

> *a simulated large aircraft breakup* - a breakup at 10,000 m (c. 33,000 ft), with an initial forward velocity of 250 m/s (c. 485 kts) and a cross/tail wind of 43 kts (decreasing with reducing altitude) adopting a wind profile given below, and
>
> *a simulated small aircraft breakup* - a breakup at 1,000 m (c. 3,250 ft), with an initial forward velocity of 60 m/s (c. 120 kts) and a light cross/tail wind of 12 kts (decreasing with reducing altitude).

The parameters varied are: breakup altitude; initial *x*-direction (aircraft track) velocity, wind direction, and wind magnitude. Drag coefficient is not studied explicitly, however, the scenarios will be calculated for a range of ballistic coefficients and hence changes in drag coefficient can be inferred by moving from one ballistic coefficient value towards the next. The wind profile used in the simulations is: 40 kts at 10,000m; 17 kts at 6,000m; 13 kts at 3,000m; and 1 kt at ground level. All wind directions are 'to' 45 degrees from aircraft track. A cubic polynomial is then fitted to this data which is equivalent to using one 'span' of the cubic spline.

Figure 3 shows the effect of altering breakup height on the final location of wreckage. The plot shows the *x* and *y* location (with the breakup occurring at 0,0 and the aircraft travelling in the positive *x*-direction i.e. up the page) for the speed and wind conditions described above. Five values of ballistic coefficient are indicated (10,000, 1,000, 100, 10 and 1 kg/m^2), and for each case the effect of increasing or reducing the breakup altitude by 10% (=1,000 m) are shown. The first point of note from Figure 3 is the scale of the wreckage distribution. Wreckage is spread over an area of 30km x 30km, with the furthest pieces having 'flown' for in excess of 30 minutes. Clearly in the case of strong winds, these timescales and distances will increase.

Figure 3 shows that for high C_B items (high mass / low drag) the effect of altitude increase or decrease is to slightly increase or decrease the 'throw' of the item. However, as C_B decreases, so the difference in ground position from the reference is increased, with a 10% increase in breakup altitude giving rise to around 6km of increased displacement. The reason for this is that the increased flight time of the low C_B particle, allows proportionally more time under the wind influence due to its low terminal velocity (≈6 m/s) compared to the high C_B particle with a high terminal velocity (>340 m/s). In addition, the low C_B particle is more greatly affected by wind.

Figure 4 shows the effect on the small aircraft breakup simulation of modifying initial forward velocity. It is clear that the lower ballistic coefficient particles (C_B <= 10) are almost entirely unaffected by the change in initial velocity, showing near identical positions for all three cases. The reason for this is that low mass, high drag components decelerate extremely rapidly after release and therefore the 'modified' initial velocity has a very short period over which to influence the behaviour of the particle; it quickly adopts the surrounding windspeed. The high ballistic coefficient particle, with high mass and low drag, are able to sustain the modified velocity for longer before finally adopting terminal velocity (if at all) and hence a larger difference is visible, along the aircraft track.

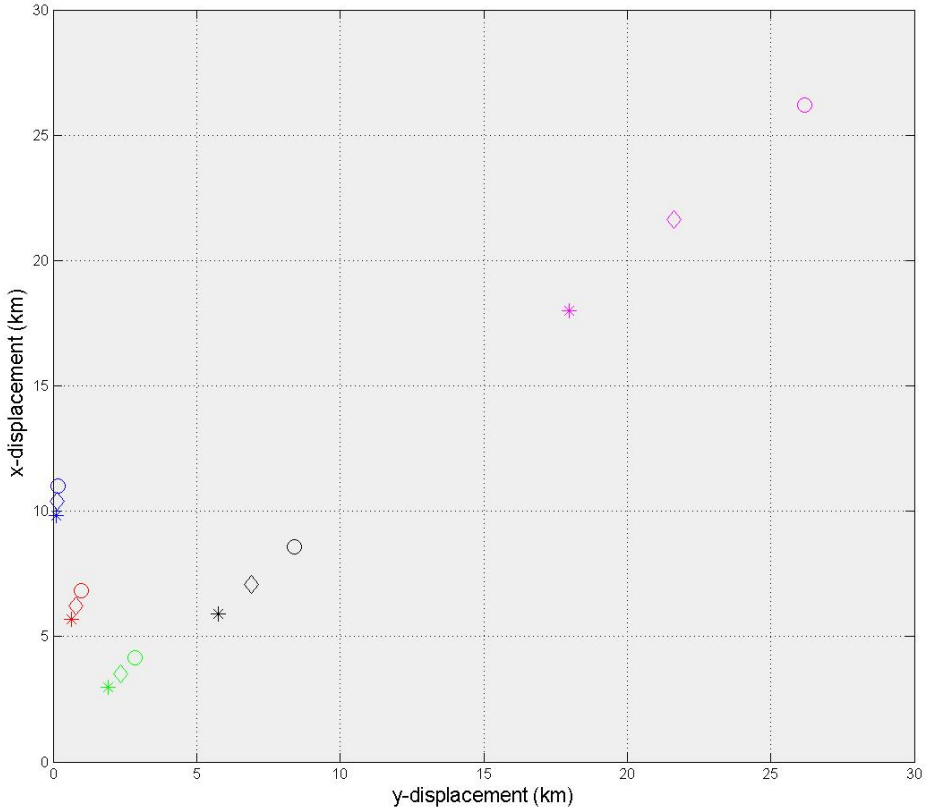

Figure 3 - The effect on final wreckage location of changing breakup altitude for a simulated large aircraft accident. C_B=10,000 ; C_B=1,000; C_B=100; C_B=10; C_B=1.
** = -10%, ◇= reference, O = +10%*

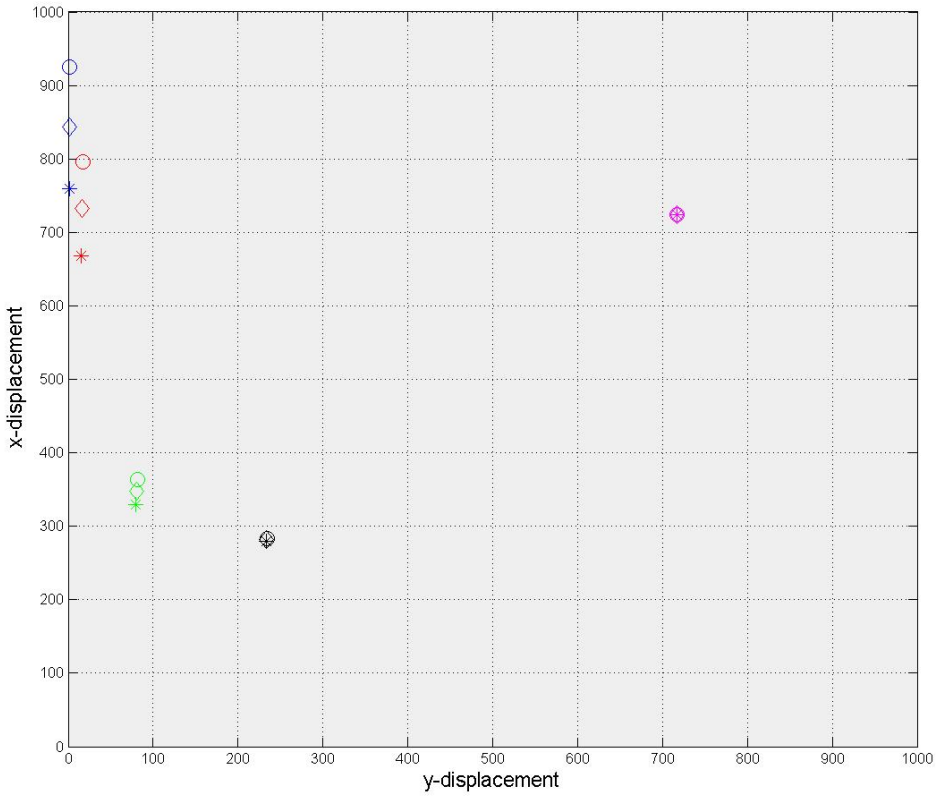

Figure 4 - The effect on final wreckage location of changing initial forward velocity for a simulated small aircraft accident. C_B=10,000 ; C_B=1,000; C_B=100; C_B=10; C_B=1.
** = -10%, ◇= reference, O = +10%*

Ground Location Difference

By performing the simulations described above, it is possible to compile data indicating the magnitude of the ground location difference for various parameters. Figure 5 shows the difference in ground location given a parameter reduction of 10% and a parameter increase of 10%. The Figure can be interpreted in a number of ways.

One option is to see which values of C_B are subject to large variation with a certain parameter. For example, both altitude and wind angle have a significant effect on low C_B items with a difference of around 5,000m compared to less than 1,000m for a high C_B item. This implies that to reduce errors for low C_B items, particular attention should be paid to breakup altitude and wind angle.

Alternatively, the Figure could be examined to establish which level of C_B is least affected by a particular parameter. For example, Figure 5 shows that low C_B items are almost independent of initial velocity changes. This implies that any low C_B discrepancies in the model fit cannot be corrected by adjusting initial velocity. Conversely, if using low C_B items to inform the modelling process, initial velocity inaccuracies will be almost completely removed and hence the other three parameters can be studied. Similarly large C_B items will tend to be independent of wind parameters. Finally, by examining the Figure, the most appropriate 'general' parameter can be assessed. In the case of Figure 5 those items with a C_B between 10^2 and 10^3 should be least sensitive to errors in the parameters investigated. Therefore, it may be most appropriate to base initial modelling estimates on 'medium' C_B values, before using the high and low values for isolating and tuning specific parameters.

Figure 5 shows that for high altitude, high initial velocity breakups, deviations in altitude and wind angle will produce the greatest effect on the ground impact location with possible errors of more than 6,000m arising from a 10% deviation. It is components with low ballistic coefficients that will be most susceptible to these errors.

Figure 6 shows the magnitude of the ground location difference for a parameter reduction of 10% and a parameter increase of 10%. Figure 6 shows similar tendencies to Figure 5. However, as with the ground location plots the magnitudes differ greatly. Maximum difference from reference are now just over 160m in comparison with 6,000m previously. This is indicative of the lower breakup altitude and shorter time of flight.

As with the large aircraft breakup, the greatest error still arises from deviations in breakup altitude and wind angle for low C_B items. However whereas for the large aircraft breakup a 10% deviation in velocity produced an error of one-sixth (1,000m) of the maximum for a high C_B item, for the small aircraft breakup this value is increased to approximately one-half of the maximum error.

For the large aircraft breakup, two C_B values were appropriate as 'general' items, but for the small aircraft breakup, a ballistic coefficient of 100 is least sensitive to deviations in the four parameters studied.

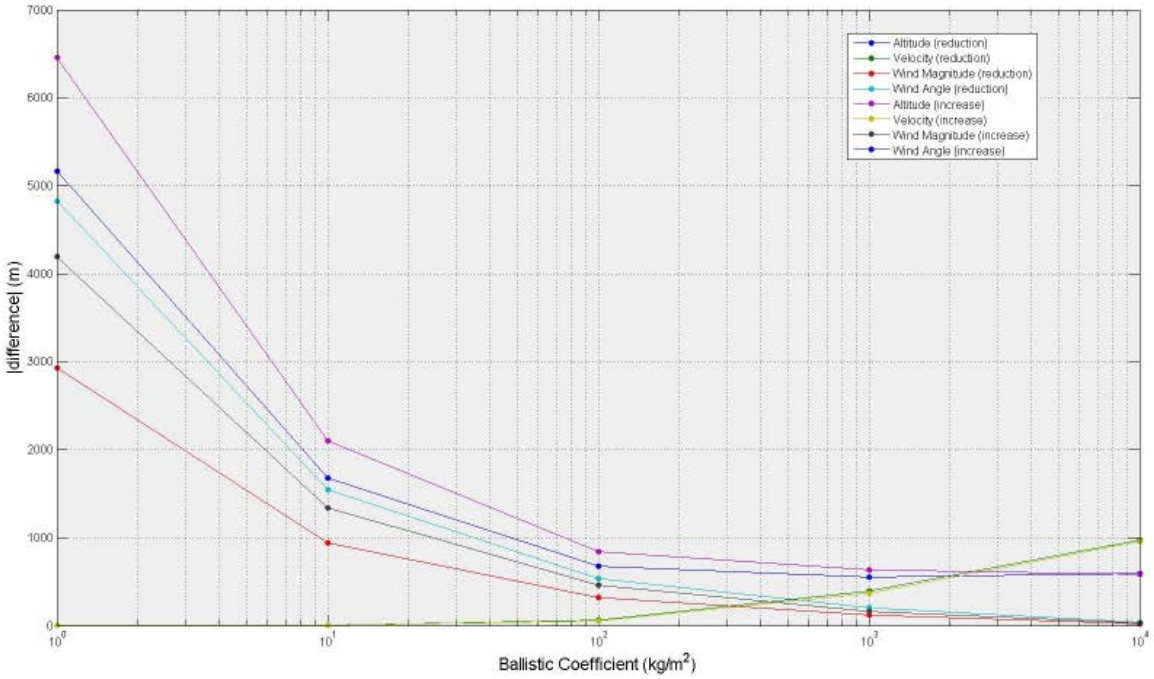

Figure 5 - Variation in magnitude of distance from position in reference case for of various parameters and C_B

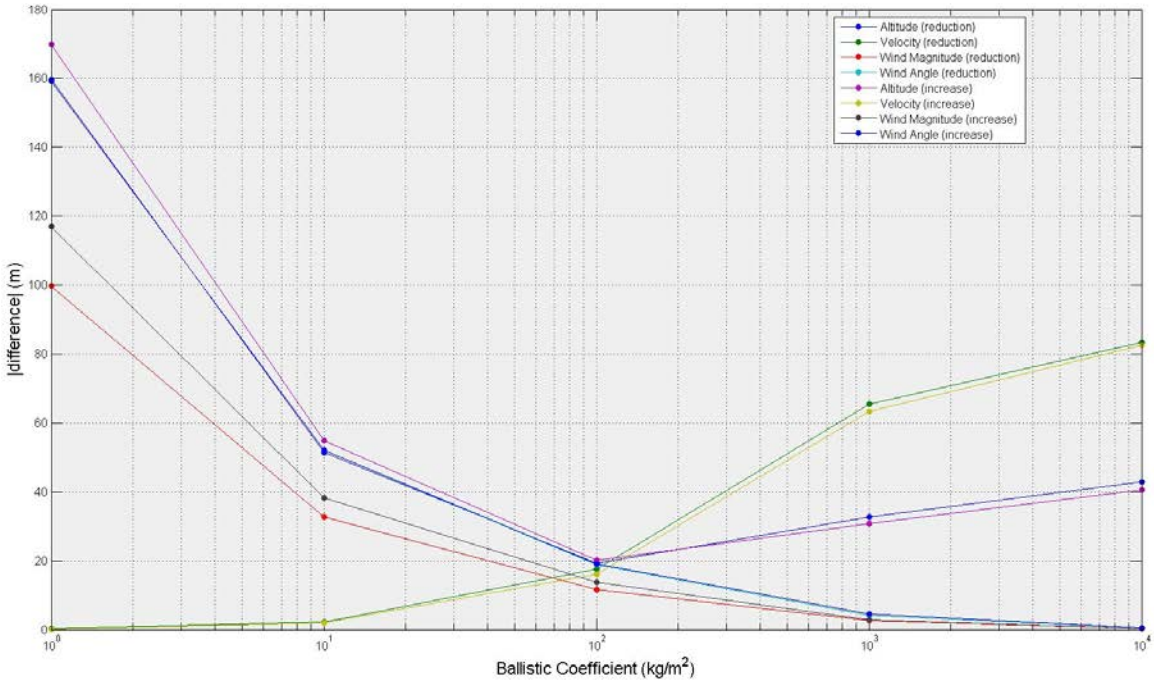

Figure X6 - Variation in magnitude of distance from position in reference case for combined of various parameters and C_B

Conclusions

Ballistic trajectory analysis has been key to many large investigations and much of the science is well understood. However, there has been no package that has incorporated variable gravity, variable density and variable wind profiles into a set of differential equations and then solved them in a robust way. This paper describes the derivation and solution of such a model and presents results gained from it. The numerical solution was validated against a simplified analytical case. Results are given for two simulated breakup cases which provide investigators with information regarding the effect on ground location for variations in four significant parameters.

The results indicate that for simulated large aircraft breakups, low ballistic coefficient items are most heavily affected by breakup altitude, wind magnitude and wind angle whereas large ballistic coefficient items are most heavily affected by breakup velocity, although to a much lesser extent (around 15% of the distance of low ballistic coefficient). For small aircraft breakups, wind angle and breakup altitude have the largest effect on low ballistic coefficient items, with velocity and altitude affecting high ballistic coefficient items to a larger extent (around 50% of low ballistic coefficient items).

References

1 Air Accidents Investigation Branch (AAIB), 1990. *Report on the accident to Boeing 747-121, N739PA at Lockerbie, Dumfrieshire, Scotland on 21 December,* Aircraft Accident Report 2/90, London: HMSO.

2 National Transportation Safety Bureau (NTSB), 2000. *In-flight Breakup Over The Atlantic Ocean Trans World Airlines Flight 800 Boeing 747-131, N93119 Near East Moriches, New York July 17, 1996*, NTSB/AAR-00/03, Washington D.C.: NTSB.

3 National Transportation Safety Committee (NTSC), 2008. *Boeing 737–4Q8 PK–KKW, Makassar strait, Sulawesi, Republic of Indonesia, 1 January 2007.* KNKT/07.01/08.01.36 Indonesia: NTSC.

4 National Transportation Safety Bureau (NTSB), 1990. *United Airlines Flight 232, McDonnell Douglas DC-10-10, Sioux Gateway Airport, Sioux City, Iowa, July 19, 1989*, NTSB/AAR-90/06, Washington D.C.: NTSB.

5 Royal Aircraft Establishment (RAE), 1946. *Note on estimation of the height and order of disintegration of an aircraft breaking up in flight by calculation of the trajectories of the pieces found in the wreckage trail,* Deptl. Note No. Acc. 146, London: HMSO.

6 Owen, J. B. B. and Grinsted, F., 1949. *The investigation of accidents involving air-frame failure,* Aeronautical Research Council R. & M. No. 2300, London: HMSO.

7 Templin, R. J. and Callan, M. M., 1956. *Generalized trajectory curves for bodies moving in air*, National Aeronautical Establishment, Note 13 (LR-159), Ottawa.

8 Braun, W., 1956. *A Method of Plotting Trajectories of Pieces from Disintegrating Aircraft*, Royal Aircraft Establishment, Accident Note No: Structures 281, London: HMSO.

9 Currie, M. M., 1960. *Generalized Tables for the Calculation of Trajectory Curves for Bodies Moving in the Air,* National Research Council of Canada, National Aeronautical Establishment, Aeronautical Report LR-277, NRC No. 6585, Ottawa.

10 Gwilt, S. R., 1961. *Trajectory Analysis in Aircraft Accident Investigation,* National Research Council of Canada, National Aeronautical Establishment, Aeronautical Report LR-310, Ottawa.

11 Waterfall, A. P., 1966. *A Computer Technique for the Analysis of Three Dimensional Ballistic Trajectory Data Including Aerodynamic Effects*, Royal Aircraft Establishment, Technical Report No. 66163, London: HMSO.

12 Boksenbom, A. S., *Graphical Trajectory Analysis,* NASA Technical Note D-64.

13 Cranfield Aviation Safety Centre, 1993. *Airshow Separation Distances*, Report for Civil Aviation Authority, Cranfield.

14 Oldham Jr., H. E., 1990. *Aircraft Debris Trajectory Analysis*, http://www.proairshow.com/aircraft_debris.htm, accessed 4th Feb 2009.

15 Bergen-Henengouwen, S. G., 1970. *Wreckage Trajectory Analysis in Aircraft Accident Investigation*, MEng thesis, Carleton University, Ottawa, Ontario.

16 Bergen-Henengouwen, S. G., 1971. *Wreckage Trajectory Analysis in Aircraft Accident Investigation*, Canadian Aeronautics and Space Journal, Nov, pp. 355-361.

17 Matteson, F. H., 1974. *Analysis of Wreckage Patterns from In-Flight Disintegrations*, Journal of Safety Research, Vol 6, No. 2, pp. 60-71.

18 Kepert, J. L., 1976. *The Use of Wreckage Trajectories in Aircraft Accident Investigation,* Defence Science and Technology Organization, Aeronautical Research Laboratories, Structures Note 427, Melbourne.

19 National Transportation Safety Bureau (NTSB), 2000. *In-flight Breakup Over The Atlantic Ocean Trans World Airlines Flight 800 Boeing 747-131, N93119 Near East Moriches, New York July 17, 1996*, Section 22A: Trajectory Study, NTSB/AAR-00/03, Washington D.C.: NTSB.

20 Kirpal, Hon'ble Mr Justice B. N., 1986 *Accident to Air India Boeing 747 Aircraft VT-EFO, "Kanishka" on 23rd June 1985*.

21 Guan, W. and Yong, K., *Ballistic Trajectory Analysis for the CI611 Accident Investigation*, Aviation Safety Council Publication

22 Khan, I. J., 1978. *Study of Trajectories of Aircraft Parts Following In-flight Breakup*, MSc Thesis, Cranfield Institute of Technology.

23 Hull, S. R., 1980. *A 3-D Trajectory Analysis of Aircraft Parts Following Inflight Break Up,* MSc thesis, Cranfield Institute of Technology.

24 Steele, R. M. G., 1983. *Trajectory Plots of Aircraft Debris Following In-flight Breakup*, MSc thesis, Cranfield Institute of Technology.

25 Anker, R. and Taylor, A. F., *The trajectories of falling parts following in-flight breakup*, ISASI forum magazine, (Proceeding of the 20th International Seminar) Vol 22, No.4 Dec 1989, pp. 133-140

26 Taylor, A. F., 1991. *The effect of wind on the wreckage trail following in-flight breakup*, Cranfield College of Aeronautics Aerogram, Vol. 6, No. 3.

27 Taylor, A. F. 1998. *The study of aircraft wreckage: the key to aircraft accident investigation*, Technology, Law and Insurance, Vol 3, pp. 129-147.

28 DTIC website http://www.dtic.mil/doctrine/jel/doddict/data/b/00611.html, accessed 16th Jan, 2012

29 International Civil Aviation Organisation ICAO), 1993. *Manual of the ICAO Standard Atmosphere extended to 80 kilometres (262 500 feet)*, 3rd Edition, Doc 7488/3.

30 http://www.virgingalactic.com/assets/downloads/Virgin_Galactic_Brochure.pdf accessed Jan 16th 2012

31 Hoerner, S. F., 1958. Fluid-dynamics Drag,

32 http://ruc.noaa.gov/ accessed 16th Jan 2012.

33 Press et al., 2007. *Numerical Recipes,* 3rd Edition, Cambridge University Press.

34 Lapidus, L. and J. H. Seinfeld, 1971. *Numerical Solution of Ordinary Differential Equations,* Academic Press.p268

35 Hall, G. and J. M. Watt, 1976. *Modern Numerical Methods for Ordinary Differential Equations,* Clarendon Press